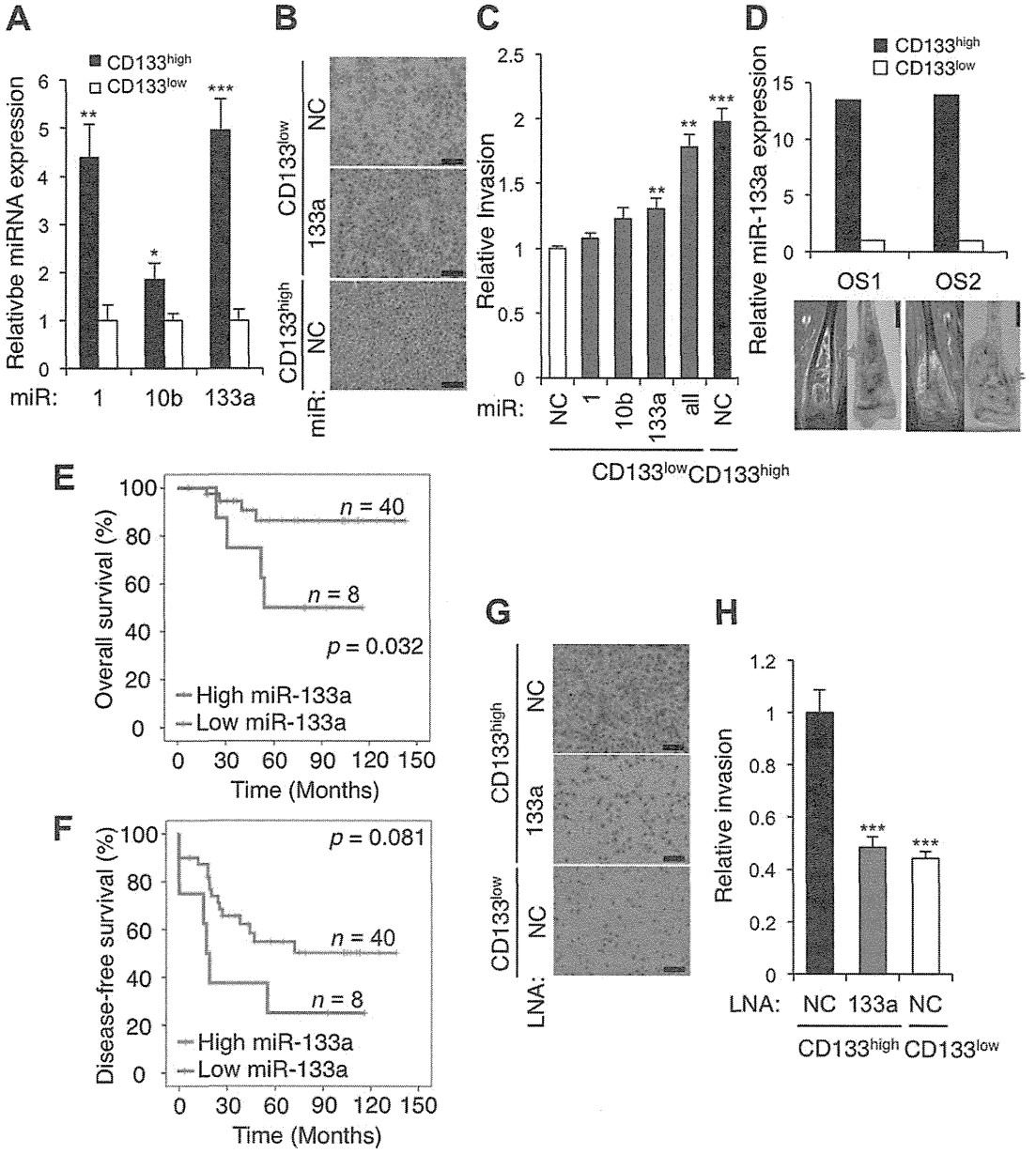

Figure 2. MiR-133a regulates cell invasion of tumor-initiating cell population within osteosarcoma and represents prognostic value. **(A):** The upregulated expression levels of miR-1, 10b, and 133a in CD133^{high} cell population. Data are presented as mean ± SD ($n = 3$ per group). *, $p < .05$; **, $p < .01$; ***, $p < .001$; Student's t test. **(B, C):** Invasion assays in purified CD133^{low} SaOS2 cells transfected with miR-1, 10b, and 133a oligos. CD133^{low} SaOS2 cell populations were transfected with miR-1, 10b, 133a, or NC mimics at a final concentration of 30 nM. At the time periods of 24 hours post-transfection, cells were seeded and cultured on the invasion chamber for 36 hours. The number of invaded cell were photographed (B) and counted (C). Scale bar = 200 μm. Data are presented as mean ± SD ($n = 3$ per group). **, $p < .01$; ***, $p < .001$, calculated with one-way ANOVA with Bonferroni's multiple comparison when compared with the CD133^{low} cell population treated with miR-NC. **(D):** The expression level of miR-133a in CD133^{high} and CD133^{low} populations of freshly resected patient biopsies. **(E, F):** The Kaplan-Meier curves for overall survival (E) and disease-free survival (F) based on the levels of miR-133a expression in 48 formalin-fixed paraffin-embedded tissues from osteosarcoma biopsy specimens, as determined using quantitative reverse transcriptase polymerase chain reaction. The overall survival rate ($p = .032$; log-rank test) and disease-free survival rate ($p = .081$; log-rank test) for osteosarcoma patients with high miR-133a expression (red line) were compared with those for patients with low miR-133a expression (green line). See also Supporting Information Figure S2B and Table S2. **(G, H):** Invasion assays in LNA-133a-treated SaOS2 CD133^{high} populations. CD133^{high} and CD133^{low} SaOS2 cell populations were isolated and transfected with LNA-133a or LNA-NC to reduce the expression of miR-133a in the CD133^{high} cell population. As a control, CD133^{low} cell populations were transfected with LNA-NC. At the time periods of 24 hours post-transfection, cells were seeded and cultured on the invasion chamber for 36 hours. The number of invaded cell were photographed (G) and counted (H). Scale bar = 200 μm. Data are presented as mean ± SD ($n = 3$ per group). ***, $p < .001$, calculated with one-way ANOVA with Bonferroni's multiple comparison when compared with the CD133^{high} cell populations treated with LNA-NC. Abbreviations: LNA, locked nucleic acid; NC, negative control.

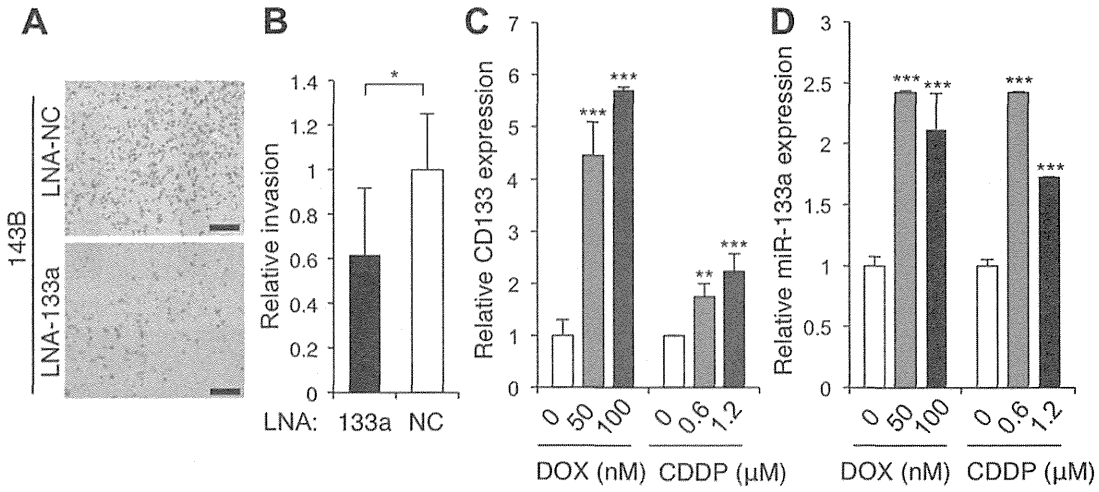

Figure 3. Chemotherapy induces the expression of miR-133a in highly malignant osteosarcoma 143B cells. **(A, B):** Invasion assay in highly metastatic osteosarcoma 143B cells treated with LNA-133a and NC. At the time periods of 24 hours post-transfection, cells were seeded and cultured on the invasion chamber for 24 hours. The number of invaded cell were photographed (A) and counted (B). Scale bar = 200 μm. Data are presented as mean ± SD ($n = 3$ per group). *, $p < .05$; Student's t test. **(C):** The induced expression of CD133 in 143B cells in the presence of chemotherapeutics (DOX and CDDP, 48 hours). Data are presented as mean ± SD ($n = 3$ per group). **, $p < .01$; ***, $p < .001$, calculated with one-way ANOVA with Bonferroni's multiple comparison when compared with untreated cells. **(D):** The induced expression of miR-133a in 143B cells in the presence of chemotherapeutics (DOX and CDDP, 48 hours). Data are presented as mean ± SD ($n = 3$ per group). ***, $p < .001$, calculated with one-way ANOVA with Bonferroni's multiple comparison when compared with untreated cells. Abbreviations: CDDP, cisplatin; DOX, doxorubicin; LNA, locked nucleic acid; NC, negative control.

The Expression Levels of MiR-133a in Osteosarcoma Cells Are Enhanced by Chemotherapy

Next, we validated the efficacy of LNA-133a on highly malignant metastatic osteosarcoma 143B cells, since SaOS2 cells represent low metastatic ability *in vivo* [42, 43]. Meanwhile, we needed to evaluate the efficacy of LNA on "bulk" 143B cells, assuming clinical situations. As a result, LNA-133a reduced the invasiveness of 143B cells (Fig. 3A, 3B) but did not influence cell proliferation (Supporting Information Fig. 5F). Since recent study has indicated a novel mechanism of chemotherapy-induced tumor progression via expansion of TIC population [44], the expression levels of CD133 and the related miR-133a within cells treated with or without chemotherapeutics were analyzed. As a result, we observed that the expression levels of miR-133a, together with CD133, were enhanced by chemotherapy. qRT-PCR analysis revealed that DOX-treated or CDDP-treated (2 days) 143B cells expressed higher levels of CD133 and miR-133a compared with untreated 143B cells (Fig. 3C, 3D). Therefore, silencing of miR-133a before or during chemotherapy may prevent the increased expression of miR-133a, which enhanced the malignant phenotypes and was induced by chemotherapeutics.

Therapeutic Administration of LNA-133a with Chemotherapy Inhibits Spontaneous Lung Metastasis and Prolongs the Survival of Osteosarcoma-Bearing Mice

To extend our *in vitro* findings and to determine whether silencing of miR-133a could be an effective therapeutic option for osteosarcomas, we next examined the effect of LNA-133a on a spontaneous lung metastasis model of osteosarcoma. Experimentally, 1.5×10^6 143B cells transfected with the firefly luciferase gene (143B-luc) were implanted orthotopically into the right proximal tibia of athymic nude mice. The implanted tumor growth and the presence of distant metastases were analyzed weekly for luciferase bioluminescence using an *in vivo* imaging system. We used a new treatment protocol (Fig. 4A) with the intravenous (i.v.) administration of LNA-133a (10 mg/kg) 24 hours before intraperitoneal (i.p.) injection of CDDP (3.5 mg/kg) to prevent the induction of malignant phenotypes by chemotherapy, which were indicated in the *in vitro* experiments. Prior to conducting these animal studies, we confirmed that miR-133a levels were reduced in osteosarcoma tissues from LNA-133a-treated mice compared with control mice (Supporting Information Fig. S6A, S6B). To assess the efficacy of our protocol, the results were compared with the results obtained for the following four control groups ($n = 10$ per group): the control saline followed by control saline group, the LNA-NC followed by control saline group, the LNA-133a followed by control saline group, and the LNA-NC followed by CDDP group. After implantation of the 143B-luc cells, five mice within each one cage were sacrificed at 3 weeks after evaluating lung metastasis by *in vivo* imaging and validated for lung metastasis formation by additional *in vivo* imaging and histological examination of the lung, whereas the other five mice in the other cage were evaluated for survival periods. The results demonstrated that the tumor expression levels of miR-133a were decreased in the presence of LNA-133a (Fig. 4B). Although tumor growth at the primary site was significantly reduced in CDDP-treated group, we identified no significant difference between LNA-133a-CDDP-treated mice and LNA-NC-CDDP-treated mice (Fig. 4C, 4D). We observed lung metastases on day 22 in nine (90%) saline-saline-treated mice, eight (80%) LNA-NC-saline-treated mice, seven (70%) LNA-133a-saline-treated mice, eight (80%) LNA-NC-CDDP-treated mice, and three (30%) LNA-133a-CDDP-

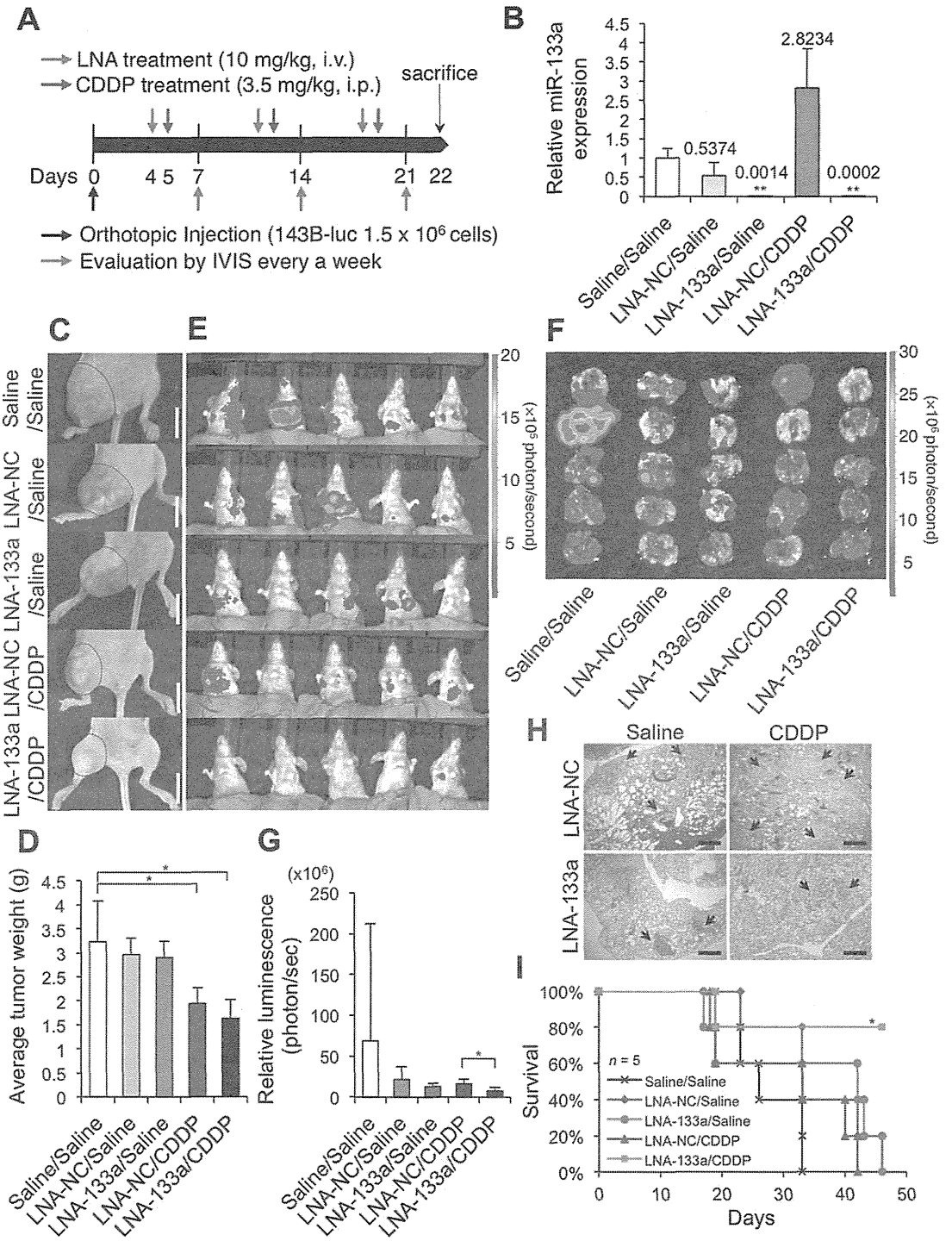

Figure 4. Therapeutic administration of LNA-133a with systemic chemotherapy inhibits osteosarcoma progression *in vivo*. **(A):** A schematic representation of the LNA-133a (red arrow) and CDDP (blue arrow) administration schedule for 143B-luc-bearing mice. **(B):** The expression levels of miR-133a in osteosarcoma tissues ($n = 5$ per group) analyzed by quantitative reverse transcriptase polymerase chain reaction. The tumors were obtained during autopsy after completion of treatment on day 22. Data are presented as mean ± SD ($n = 5$ per group). **, $p < .01$, as compared to control saline-treated group; Student's *t* test. **(C, D):** Tumors at the primary site of each treatment group measured on day 22. The macroscopic appearances of 143B-luc tumors in each group of mice on day 22 are shown (C). The tumor masses outlined by a dotted line. Scale bar = 10 mm. The 143B-luc tumors from each group of mice were weighed on day 22 (D). Data are presented as mean ± SD ($n = 5$ per group). *, $p < .05$, as compared to control saline-treated group; Student's *t* test. **(E–G):** The lung metastases of each treatment group measured on day 22 using an IVIS. The representative luminescence of the chest regions in each group of mice was determined (E). For each mouse that was sacrificed to validate the lung metastases, each lung was re-evaluated using IVIS (F). The representative average luminescence of the chest region in each group of mice ($n = 10$) was compared among the treatment groups (G). Data are presented as mean ± SD ($n = 5$ per group). *, $p < .05$, as compared with LNA-NC/CDDP and LNA-133a/CDDP group; Student's *t* test. **(H):** Lung metastases validated by H&E staining. Black arrow represents metastatic foci in the lung. Scale bars = 500 μm. **(I):** Survival curves for each group of mice by Kaplan-Meier analysis. Log-rank test was performed between LNA-NC/CDDP group (blue line) and LNA-133a/CDDP group (red line) (*, $p = .026$). Abbreviations: CDDP, cisplatin; IVIS, *in vivo* imaging system; LNA, locked nucleic acid; NC, negative control.

treated mice ($n = 10$; Fig. 4E, 4F). We observed the decreased signal intensity in the chest regions of LNA-133a-CDDP-treated mice compared to those of LNA-NC-CDDP-treated mice (Fig. 4G). Both the number and size of lung metastases were validated by histopathological examination (Fig. 4H). We found low cell concentration in lung metastatic foci of CDDP-treated groups, indicating therapeutic effect of chemotherapy, and identified smallest number of osteosarcoma metastatic foci in the lung of LNA-133a-CDDP-treated mice. Furthermore, LNA-133a-CDDP-treated mice showed longest survival periods among the five groups in Kaplan-Meier analysis (log-rank test, $p = .026$; Fig. 4I). Despite the conserved sequence of mature hsa-miR-133a and mmu-miR-133a (Supporting Information Fig. S7A), all mice exhibited minimal toxic effects on various tissues, including the heart, liver, skeletal muscle, and blood test, during the observation period (Supporting Information Fig. S7B–S7H, S8A–S8I). Thus, systemic administration of LNA-133a was effective for the suppression of lung metastases in a xenograft model of a highly metastatic osteosarcoma in the presence of CDDP.

Multiple Target Genes of MiR-133a Function as Regulators of Cell Invasion and Closely Correlate with Clinical Behavior of Osteosarcoma

We demonstrated that miR-133a regulated the malignancy of $CD133^{high}$ osteosarcoma cell population and that silencing of miR-133a expression with chemotherapeutics inhibited the osteosarcoma metastasis *in vivo*. Next, to understand the molecular mechanism regulated by miR-133a in the tumor-initiating population, we performed mRNA expression profiling using two different microarray analyses together with *in silico predictions* (Supporting Information Fig. S9A). We detected 1,812 genes that were downregulated by at least 1.2-fold in the first microarray analysis, which was performed from total RNA collected from SaOS2 $CD133^{low}$ cells transduced with miR-133a or NC. Furthermore, 4,976 genes were upregulated by at least 2-fold in the second microarray analysis of mRNA expression using RNA collected using anti-Argonaute 2 antibody immunoprecipitation (Ago2 IP) in $CD133^{low}$ cells transduced with miR-133a or NC. Subsequently, 226 genes were collected using both methods, and 20 genes were identified in TargetScanHuman 6.0, a publicly available *in silico* database (Fig. 5A). Overall, 10 putative miR-133a target genes were selected from these combined data, and we reduced the expression of these molecules using an siRNA-induced gene knockdown system to investigate whether these candidates are functionally important targets of miR-133a in osteosarcoma cells. As a result, the knockdown of four genes (*SGMS2*, *UBA2*, *SNX30*, and *ANXA2*) enhanced the invasiveness of $CD133^{low}$ SaOS2 cells (Fig. 5B). To validate whether these molecules are regulated by miR-133a, we cloned the 3′ UTR fragment (Fig. 5C) containing the putative miR-133a binding sites downstream of a luciferase coding sequence and performed cotransfection of the luciferase reporter and miR-133a oligos in SaOS2 cells. Luciferase activity levels were reduced by approximately 36%–55% in the cells cotransfected with miR-133a compared with the cells cotransfected with the NC oligos (Fig. 5D). Consequently, *SGMS2*, *UBA2*, *SNX30*, and *ANXA2* functioned as direct targets of miR-133a. Indeed, these molecules have been suggested to have antitumor function in the other types of tumors [45–47]. Among them, *ANXA2* is downregulated in osteosarcoma metastases compared to primary site [48]. The expression levels of these targets were decreased in $CD133^{high}$ cells (Supporting Information Fig. S9B) and reduced via miR-133a upregulation in $CD133^{low}$ cells (Supporting Information Fig. S9C). The increased expression levels of the targets after silencing of miR-133a were confirmed by immunohistochemistry of LNA-treated tumors and qRT-PCR (Fig. 5E, 5F; Supporting Information Fig. S9D). Taken together, LNA-133a was found to inhibit cell invasion of the malignant cell population of osteosarcoma through multiple molecular pathways. Finally, we observed a strikingly close correlation between these mRNA expression levels of the miR-133a targets and osteosarcoma patient prognosis (Fig. 6A–6D). Patients with higher expression levels of these targets significantly survived longer than those with lower expression levels. These results would support the importance of regulating the expression of miR-133a during current osteosarcoma treatment, providing insight into the development of more effective therapies against osteosarcoma.

Discussion

Cancer researchers today are confronted with how to overcome the natural resistance and the acquired resistance of cancer cells within tissue, despite the many cancer treatment options. The CSC or TIC hypothesis has been an attractive model to account for the functional heterogeneity that is commonly observed in solid tumors [7]. To characterize and eliminate the malignant cells in cancers that follow this model, it has been necessary to focus on the small subpopulations of tumorigenic cells [49]. Tremendous efforts and evidence have accumulated to identify these subpopulations [13–18, 20, 21]. However, these markers are generally difficult to be targeted because of their distribution on the normal stem cells. For example, targeting CD133 seems unsafe because this cell-surface protein is primarily expressed in stem and progenitor cells [50] such as the embryonic epithelium [51], brain stem cells [52], and hematopoietic stem cells [32, 53]. Therefore, the molecular mechanisms underlying the malignant phenotypes must be elucidated to avoid toxicities, which have not been fully accomplished. On the basis of our results, we propose novel therapeutic strategies, beyond the use of traditional antiproliferative agents, for suppression of the highly malignant cell population within osteosarcoma using RNAi therapeutics, which is expected to be the "next-generation" anticancer strategy. Subsequently, we present four novel discoveries that were identified in a preclinical trial of novel therapeutic strategies against osteosarcoma.

First, we identified human miR-133a as a key regulator of the malignant tumor-initiating phenotypes of osteosarcoma. The other miRNAs that might regulate these phenotypes included miR-1 and miR-10b. The human miRNA hsa-miR-10b is also positively associated with high-grade malignancies, including breast cancer [54, 55], pancreatic adenocarcinomas [56], and glioblastomas [57]. However, the importance of miR-10b in sarcoma development has not been previously reported. In our experiment, miR-10b regulated, less than miR-133a, the cell invasion of osteosarcoma. The human miRNAs hsa-miR-1 and hsa-miR-133a are located on the same chromosomal region in a so-called cluster. We found that miR-

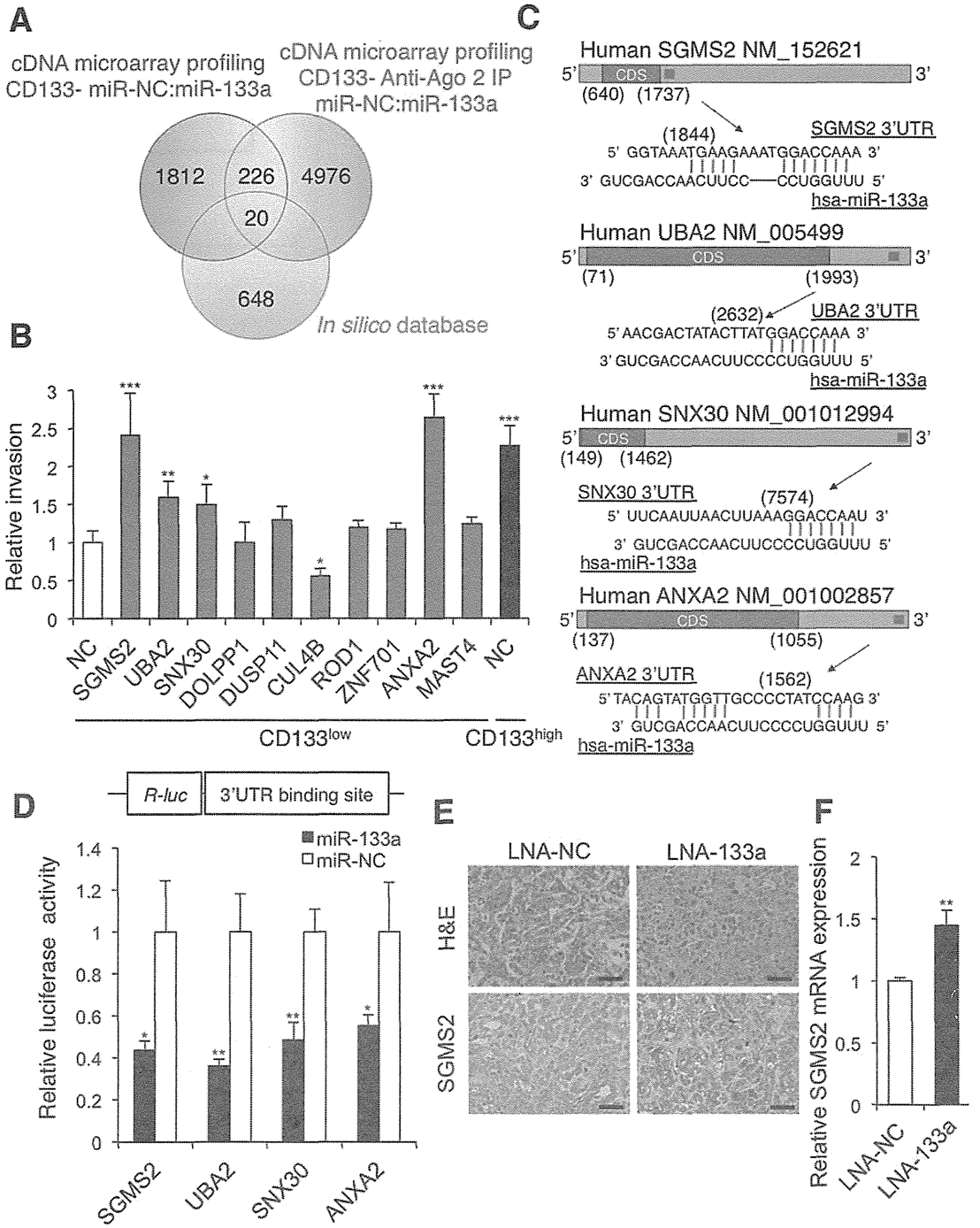

Figure 5. The direct target genes of miR-133a regulate malignant phenotypes of osteosarcoma. **(A):** A Venn diagram of the candidate target mRNAs of miR-133a based on the cDNA microarrays and *in silico* database. **(B):** Invasion assays performed using SaOS2 cells 24 hours post-transfection of the 10 siRNAs. $CD133^{high}$ and $CD133^{low}$ SaOS2 cell populations were isolated using flow cytometry and transfected with 10 siRNAs against the identified genes in **(A)**. Data are presented as mean ± SD ($n = 3$ per group). *, $p < .05$; **, $p < .01$; ***, $p < .001$, calculated with one-way ANOVA with Bonferroni's multiple comparison when compared with the $CD133^{low}$ cells transfected with nontargeting siRNA. **(C):** Schematics of the miR-133a binding site within the 3′ UTR of the target mRNAs. **(D):** Luciferase activities measured by cotransfecting miR-133a oligos and the luciferase reporters. Data are presented as mean ± SD ($n = 3$ per group). *, $p < .05$; **, $p < .01$; Student's *t* test. **(E, F):** Representative SGMS2 immunohistochemistry images of 143B-luc tumor sections (E) and the relative SGMS2 expression of 143B-luc tumor sections performed by quantitative reverse transcriptase polymerase chain reaction analysis (F). Scale bars = 50 μm. Data are presented as mean ± SD ($n = 3$ per group). **, $p < .01$; Student's *t* test. Abbreviations: ANXA2, annexin A2; IP, immunoprecipitation; LNA, locked nucleic acid; NC, negative control; SGMS2, sphingomyelin synthase 2; SNX30, sorting nexin family member 30; UTR, untranslated region; UBA2, ubiquitin-like modifier activating enzyme 2.

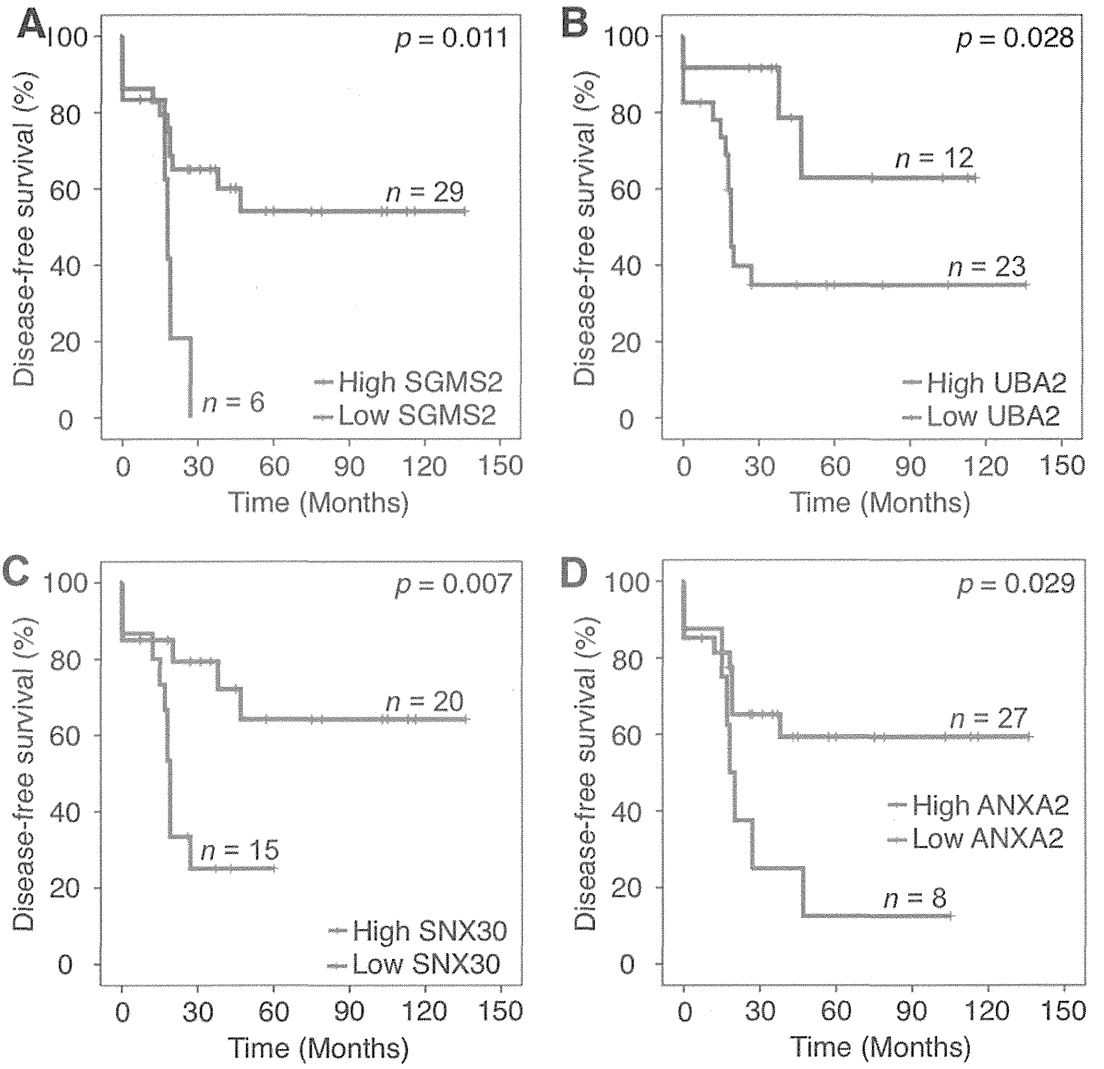

Figure 6. The low expression levels of miR-133a target genes correlate with poor survival of osteosarcoma patients. **(A–D):** Kaplan-Meier survival curves of disease-free survival according to the expression levels of the miR-133a target genes including *SGMS2* (A), *UBA2* (B), *SNX30* (C), *ANXA2* (D) in 35 patient biopsy samples. The optimal cutoff points were determined by the Youden index under the receiver-operating characteristic curve. The statistical significance of differences were determined by the log-rank test. Abbreviations: ANAX2, annexin A2; SGMS2, sphingomyelin synthase 2; SNX30, sorting nexin family member 30; UTR, untranslated region; UBA2, ubiquitin-like modifier activating enzyme 2.

1 showed only a little efficacy on invasiveness in osteosarcoma cells. The most important miRNA that could regulate the multiple phenotypes of osteosarcoma-initiating cells was miR-133a. Although miR-1 and miR-133a correlate with the proliferation of muscle progenitor cells and promote myogenesis [58], their importance in muscle physiology and disease remains unclear [59]. Indeed, miR-133a may be dispensable for the normal development and function of skeletal muscle because skeletal muscle development and function appears unaffected in miR-133a transgenic mice [59]. In this study, silencing of miR-133a had no toxic effect on muscle, including heart and skeletal muscle *in vivo* (Supporting Information Fig. S7E–S7G). Because the upregulation of miR-133a in osteosarcoma cells did not regulate the expression levels of CD133, we determined that it regulated multiple pathways that are not upstream of CD133 expression. Since the inducible factors of CD133 in osteosarcoma have not been cleared, further investigation of the relationship between the tumor microenvironment and CD133 might be warranted. Indeed, the activation of the hypoxia signaling pathway, for example, has been reported to trigger many pathways important for stem cell maintenance [60–62].

Second, we determined the efficacy of LNA technology, an antisense miRNA inhibitor oligonucleotide, as therapeutics against solid cancer. To date, the efficacy of LNAs against human disease has been reported in hepatitis and lymphoma. For example, LNA-antimiR-122 (Miravirsen, Santaris Pharma, San Diego, CA) effectively treats chimpanzees infected with

hepatitis C virus without any observable resistance or physiological side effects [63]. This treatment has advanced to phase II clinical trials, which emphasizes the strengths of LNA-mediated miR-122 silencing, including high efficacy and good tolerability without adverse effects [64]. The other report represents the preclinical trial of LNA-mediated miR-155 silencing against low-grade B-cell lymphoma [65]. Therefore, our preclinical study contributes to the broad application of LNA treatment including solid tumors. While an effective drug delivery system has been the most challenging remaining consideration for the successful translation of RNAi to the clinic for broad use in patients, the systemic administration of LNA-133a did not need assistance of drug delivery system to decrease the expression of miR-133a. These results are consistent with the results of the trial of LNA against HCV infection, in which the LNA was injected via subcutaneous injection. This preclinical trial will not only provide a novel treatment strategy against osteosarcoma but will also support a wide range of LNA applications against cancers that require the silencing of specific miRNAs.

Third, the multiple targets of miR-133a were identified to have antitumor functions against osteosarcoma with clinical relevance. Using an siRNA-induced gene knockdown system and a 3′ UTR luciferase reporter assay, we identified *SGMS2*, *UBA2*, *SNX30*, and *ANXA2* as novel antitumor molecules of osteosarcoma. Some of these molecules have been reported their association with other cancers but not for osteosarcoma. *SGMS2*, located on 4q25, is an enzyme that catalyzes the conversion of phosphatidylcholine and ceramide to sphingomyelin and diacylglycerol [66]. The specific activation of *SGMS2* explains the ability of this gene to trigger cell cycle arrest, cell differentiation, and autophagy or apoptosis in cancer cells [47]. *UBA2*, located on 19q12, forms a heterodimer that functions as a small ubiquitin-like modifier (SUMO)-activating enzyme for the sumoylation of proteins [67]. Conjugating SUMO-1, one of the four SUMO isoforms, to wild-type p53 increases the transactivation ability of p53 [45]. *SNX30*, located on 9q32, may mediate membrane association either through the lipid-binding PX domain (a phospholipid-binding motif) or protein-protein interactions. Although *SNX30* has not been well studied in cancer, loss of *SNX1*, one of the *SNX* families, plays a significant role in the development and aggressiveness of human colon cancer, at least partially through increased signaling from the endosomes [46]. In this study, we found correlations between the expression of *SGMS2*, *UBA2*, and *SNX30* and osteosarcoma cell invasion, as well as a close correlation with the prognosis of osteosarcoma patients. *ANXA2*, located on 15q22, belongs to a large family of diverse proteins that are characterized by conserved annexin repeat domains and the ability to bind negatively charged phospholipids in a calcium-dependent manner [68]. The expression levels of *ANXA2* are decreased in a subset of human OS metastases and metastatic lines [69], but the actual role of *ANXA2* in suppressing OS metastasis has remained unclear [37], which was identified as a regulator of osteosarcoma cell invasion. In this study, we were unable to identify the target genes of miR-133a that were involved in cellular proliferation, which is a general characteristic of TICs. This result may provide one explanation for why the difference in the proliferation rate of the $CD133^{high}$ and $CD133^{low}$ cell populations was relatively small. Another reason for this difference may have been heterogeneiety even within the $CD133^{high}$ cell population. Further investigation of additional markers might shed further light on the mechanisms underlying these phenotypes.

The most interesting and surprising results were the close correlations between the clinical behaviors of osteosarcoma and the expression of the factors associated with malignant tumor-initiating phenotypes, including CD133, miR-133a, and the target genes of miR-133a. These results support the importance of silencing of miR-133a during osteosarcoma treatment. Indeed, the target molecules of miR-133a were found to be significant and novel prognostic factors for osteosarcoma patients. Further analyses of these factors, including *SGMS2*, *UBA2*, and *SNX30*, would allow a better understanding of the molecular mechanisms that regulate osteosarcoma progression.

Overall, our study represents a novel approach for the use of RNAi therapeutics against the lethal phenotype of osteosarcoma. To the best of our knowledge, this study is the first preclinical trial of RNAi therapy overcoming the sarcoma malignancy. We found that miR-133a, which was induced by chemotherapy treatment, is a key regulator of cell invasion of the malignant cell population within osteosarcoma. In a preclinical *in vivo* experiment, systemic administration of LNA-133a with chemotherapy suppressed the osteosarcoma metastasis via the multiple pathways without any significant toxicity. Silencing of miR-133a may therefore represent a novel therapeutic strategy against osteosarcoma, which would lead to an improvement in the prognosis of osteosarcoma patients.

Conclusion

Silencing of miR-133a reduced the malignancy of $CD133^{high}$ osteosarcoma-initiating cell population through restoring the expression of multiple target genes. Systemic administration of LNA-133a with CDDP reduced lung metastasis and prolonged the survival of osteosarcoma-bearing mice. A clinical study revealed that high miR-133a expression levels within the patient biopsy specimens were significantly correlated with poor prognosis, providing the importance of regulating miR-133a levels in osteosarcoma for more efficient therapy in future.

Acknowledgments

We thank T. Yamada for the cDNA library of osteosarcoma clinical samples. We also thank A. Inoue for her technical work. This work was supported in part by a grant-in-aid for the Third-Term Comprehensive 10-Year Strategy for Cancer Control of Japan, the Program for Promotion of Fundamental Studies in Health Sciences of the National Institute of Biomedical Innovation of Japan (NiBio), and a grant-in-aid for Scientific Research on Applying Health Technology from the Ministry of Health, Labor and Welfare of Japan.

Author contributions

T.F.: performed the experimental work, data analysis, and writing of the draft of the manuscript; T.K., K.H., and Y.Y.:

provided the technical skills for the *in vitro* assay; N.K. and R.T.: participated in the conception, design, and coordination of the study; F.T.: provided the technical skills for the *in vivo* LNA delivery; D.K., I.K., A.Y., and E.K.: provided osteosarcoma biopsy samples and their information; H.I.: provided osteosarcoma cell lines from clinical samples resected at the National Cancer Center Hospital of Japan. A.K. and T.O.: initiated the project and provided helpful discussion. The manuscript was finalized by T.O. with the assistance of all authors.

Disclosure of Potential Conflicts of Interest

The authors indicate no potential conflicts of interest.

References

1 Aogi K, Woodman A, Urquidi V et al. Telomerase activity in soft-tissue and bone sarcomas. Clin Cancer Res 2000;6:4776–4781.

2 Fletcher CD. The evolving classification of soft tissue tumours: An update based on the new WHO classification. Histopathology 2006;48:3–12.

3 Naka N, Takenaka S, Araki N et al. Synovial sarcoma is a stem cell malignancy. Stem Cells 2010;28:1119–1131.

4 Reya T, Morrison SJ, Clarke MF et al. Stem cells, cancer, and cancer stem cells. Nature 2001;414:105–111.

5 Clarke MF, Dick JE, Dirks PB et al. Cancer stem cells—Perspectives on current status and future directions: AACR Workshop on cancer stem cells. Cancer Res 2006;66: 9339–9344.

6 Clevers H. The cancer stem cell: Premises, promises and challenges. Nat Med 2011;17:313–319.

7 Visvader JE, Lindeman GJ. Cancer stem cells in solid tumours: Accumulating evidence and unresolved questions. Nat Rev Cancer 2008;8:755–768.

8 Allison DC, Carney SC, Ahlmann ER et al. A meta-analysis of osteosarcoma outcomes in the modern medical era. Sarcoma 2012; 2012:704872.

9 Kawaguchi N, Ahmed AR, Matsumoto S et al. The concept of curative margin in surgery for bone and soft tissue sarcoma. Clin Orthop Relat Res 2004:165–172.

10 Gupta A, Meswania J, Pollock R et al. Non-invasive distal femoral expandable endoprosthesis for limb-salvage surgery in paediatric tumours. J Bone Joint Surg 2006;88: 649–654.

11 Bacci G, Rocca M, Salone M et al. High grade osteosarcoma of the extremities with lung metastases at presentation: Treatment with neoadjuvant chemotherapy and simultaneous resection of primary and metastatic lesions. J Surg Oncol 2008;98:415–420.

12 Halldorsson A, Brooks S, Montgomery S et al. Lung metastasis 21 years after initial diagnosis of osteosarcoma: A case report. J Med Case Rep 2009;3:9298.

13 Adhikari AS, Agarwal N, Wood BM et al. CD117 and Stro-1 identify osteosarcoma tumor-initiating cells associated with metastasis and drug resistance. Cancer Res 2010; 70:4602–4612.

14 Basu-Roy U, Seo E, Ramanathapuram L et al. Sox2 maintains self renewal of tumor-initiating cells in osteosarcomas. Oncogene 2012;31:2270–2282.

15 Gibbs CP, Kukekov VG, Reith JD et al. Stem-like cells in bone sarcomas: Implications for tumorigenesis. Neoplasia 2005;7:967–976.

16 Levings PP, McGarry SV, Currie TP et al. Expression of an exogenous human Oct-4 promoter identifies tumor-initiating cells in osteosarcoma. Cancer Res 2009;69:5648–5655.

17 Siclari VA, Qin L. Targeting the osteosarcoma cancer stem cell. J Orthop Surg Res 2010;5:78.

18 Tirino V, Desiderio V, d'Aquino R et al. Detection and characterization of CD133+ cancer stem cells in human solid tumours. PloS one 2008;3:e3469.

19 Tirino V, Desiderio V, Paino F et al. Human primary bone sarcomas contain CD133+ cancer stem cells displaying high tumorigenicity in vivo. FASEB J 2011;25: 2022–2030.

20 Wilson H, Huelsmeyer M, Chun R et al. Isolation and characterisation of cancer stem cells from canine osteosarcoma. Vet J 2008; 175:69–75.

21 Wu C, Wei Q, Utomo V et al. Side population cells isolated from mesenchymal neoplasms have tumor initiating potential. Cancer Res 2007;67:8216–8222.

22 Gregory RI, Shiekhattar R. MicroRNA biogenesis and cancer. Cancer Res 2005;65: 3509–3512.

23 Ambros V. microRNAs: Tiny regulators with great potential. Cell 2001;107:823–826.

24 Calin GA, Croce CM. MicroRNA signatures in human cancers. Nat Rev Cancer 2006;6:857–866.

25 Esquela-Kerscher A, Slack FJ. Oncomirs—MicroRNAs with a role in cancer. Nat Rev Cancer 2006;6:259–269.

26 Ma S, Tang KH, Chan YP et al. miR-130b Promotes CD133(+) liver tumor-initiating cell growth and self-renewal via tumor protein 53-induced nuclear protein 1. Cell Stem Cell 2010;7:694–707.

27 Calin GA, Ferracin M, Cimmino A et al. A MicroRNA signature associated with prognosis and progression in chronic lymphocytic leukemia. New Engl J Med 2005;353:1793–1801.

28 Jiang J, Gusev Y, Aderca I et al. Association of microRNA expression in hepatocellular carcinomas with hepatitis infection, cirrhosis, and patient survival. Clin Cancer Res 2008;14:419–427.

29 Kawai A, Ozaki T, Ikeda S et al. Two distinct cell lines derived from a human osteosarcoma. J Cancer Res Clin Oncol 1989;115: 531–536.

30 Osaki M, Takeshita F, Sugimoto Y et al. MicroRNA-143 regulates human osteosarcoma metastasis by regulating matrix metalloprotease-13 expression. Mol Ther 2011;19:1123–1130.

31 Youden W. Index for rating diagnostic tests. Cancer 1950;3:32–35.

32 Gires O. Lessons from common markers of tumor-initiating cells in solid cancers. Cell Mol Life Sci 2011;68:4009–4022.

33 Cao Y, Zhou Z, de Crombrugghe B et al. Osterix, a transcription factor for osteoblast differentiation, mediates antitumor activity in murine osteosarcoma. Cancer Res 2005;65: 1124–1128.

34 de Crombrugghe B, Lefebvre V, Behringer RR et al. Transcriptional mechanisms of chondrocyte differentiation. Matrix Biol 2000;19:389–394.

35 Ducy P, Zhang R, Geoffroy V et al. Osf2/Cbfa1: A transcriptional activator of osteoblast differentiation. Cell 1997;89:747–754.

36 Nakashima K, Zhou X, Kunkel G et al. The novel zinc finger-containing transcription factor osterix is required for osteoblast differentiation and bone formation. Cell 2002;108: 17–29.

37 Tang N, Song WX, Luo J et al. Osteosarcoma development and stem cell differentiation. Clin Orthop Relat Res 2008;466:2114–2130.

38 Croce CM. Causes and consequences of microRNA dysregulation in cancer. Nat Rev. Genet 2009;10:704–714.

39 Elmen J, Lindow M, Schutz S et al. LNA-mediated microRNA silencing in non-human primates. Nature 2008;452:896–899.

40 Haraguchi T, Nakano H, Tagawa T et al. A potent 2′-O-methylated RNA-based microRNA inhibitor with unique secondary structures. Nucleic Acids Res 2012;40:e58.

41 Obad S, dos Santos CO, Petri A et al. Silencing of microRNA families by seed-targeting tiny LNAs. Nat Genet 2011;43:371–378.

42 Dass CR, Ek ET, Choong PF. Human xenograft osteosarcoma models with spontaneous metastasis in mice: Clinical relevance and applicability for drug testing. J Cancer Res Clin Oncol 2007;133:193–198.

43 Kimura K, Nakano T, Park Y-B et al. Establishment of human osteosarcoma cell lines with high metastatic potential to lungs and their utilities for therapeutic studies on metastatic osteosarcoma. Clin Exp Metastasis 2002;19:477–486.

44 Tsuchida R, Das B, Yeger H et al. Cisplatin treatment increases survival and expansion of a highly tumorigenic side-population fraction by upregulating VEGF/Flt1 autocrine signaling. Oncogene 2008;27:3923–3934.

45 Gostissa M, Hengstermann A, Fogal V et al. Activation of p53 by conjugation to the ubiquitin-like protein SUMO-1. EMBO J 1999; 18:6462–6471.

46 Nguyen LN, Holdren MS, Nguyen AP et al. Sorting nexin 1 down-regulation promotes colon tumorigenesis. Clin Cancer Res 2006;12:6952–6959.

47 Ségui B, Andrieu-Abadie N, Jaffrézou J-P et al. Sphingolipids as modulators of cancer cell death: Potential therapeutic targets. Biochim Biophys Acta 2006;1758:2104–2120.
48 Gillette JM, Chan DC, Nielsen-Preiss SM. Annexin 2 expression is reduced in human osteosarcoma metastases. J Cell Biochem 2004;92:820–832.
49 Shackleton M, Quintana E, Fearon ER et al. Heterogeneity in cancer: Cancer stem cells versus clonal evolution. Cell 2009;138: 822–829.
50 Yin AH, Miraglia S, Zanjani ED et al. AC133, a novel marker for human hematopoietic stem and progenitor cells. Blood 1997;90:5002–5012.
51 Marzesco AM, Janich P, Wilsch-Brauninger M et al. Release of extracellular membrane particles carrying the stem cell marker prominin-1 (CD133) from neural progenitors and other epithelial cells. J Cell Sci 2005;118:2849–2858.
52 Uchida N, Buck DW, He D et al. Direct isolation of human central nervous system stem cells. Proc Natl Acad Sci USA 2000;97: 14720–14725.
53 Freund D, Bauer N, Boxberger S et al. Polarization of human hematopoietic progenitors during contact with multipotent mesenchymal stromal cells: Effects on proliferation and clonogenicity. Stem Cells Dev 2006;15: 815–829.
54 Ma L, Reinhardt F, Pan E et al. Therapeutic silencing of miR-10b inhibits metastasis in a mouse mammary tumor model. Nat Biotechnol 2010;28:341–347.
55 Ma L, Teruya-Feldstein J, Weinberg RA. Tumour invasion and metastasis initiated by microRNA-10b in breast cancer. Nature 2007; 449:682–688.
56 Preis M, Gardner TB, Gordon SR et al. MicroRNA-10b expression correlates with response to neoadjuvant therapy and survival in pancreatic ductal adenocarcinoma. Clin Cancer Res 2011;17:5812–5821.
57 Gabriely G, Yi M, Narayan RS et al. Human glioma growth is controlled by microRNA-10b. Cancer Res 2011;71:3563–3572.
58 Chen JF, Mandel EM, Thomson JM et al. The role of microRNA-1 and microRNA-133 in skeletal muscle proliferation and differentiation. Nat Genet 2006;38:228–233.
59 Deng Z, Chen JF, Wang DZ. Transgenic overexpression of miR-133a in skeletal muscle. BMC Musculoskelet Disord 2011;12:115.
60 Heddleston JM, Li Z, Lathia JD et al. Hypoxia inducible factors in cancer stem cells. Br J Cancer 2010;102:789–795.
61 Iida H, Suzuki M, Goitsuka R et al. Hypoxia induces CD133 expression in human lung cancer cells by up-regulation of OCT3/4 and SOX2. Int J Oncol 2012;40:71–79.
62 Soeda A, Park M, Lee D et al. Hypoxia promotes expansion of the CD133-positive glioma stem cells through activation of HIF-1alpha. Oncogene 2009;28:3949–3959.
63 Lanford RE, Hildebrandt-Eriksen ES, Petri A et al. Therapeutic silencing of microRNA-122 in primates with chronic hepatitis C virus infection. Science 2010;327:198–201.
64 Kim M, Kasinski AL, Slack FJ. MicroRNA therapeutics in preclinical cancer models. Lancet Oncol 2011;12:319–321.
65 Zhang Y, Roccaro AM, Rombaoa C et al. LNA-mediated anti-miR-155 silencing in low-grade B-cell lymphomas. Blood 2012;120: 1678–1686.
66 Huitema K, van den Dikkenberg J, Brouwers JFHM et al. Identification of a family of animal sphingomyelin synthases. EMBO J 2004;23:33–44.
67 Hay RT. SUMO. A history of modification. Mol Cell 2005;18:1–12.
68 Balch C, Dedman JR. Annexins II and V inhibit cell migration. Exp Cell Res 1997;237: 259–263.
69 Mintz MB, Sowers R, Brown KM et al. An expression signature classifies chemotherapy-resistant pediatric osteosarcoma. Cancer Res 2005;65:1748–1754.

See www.StemCells.com for supporting information available online.

J Orthop Sci (2014) 19:832–837
DOI 10.1007/s00776-013-0378-1

CASE REPORT

Long-term follow-up of resection–replantation for sarcoma in the distal radius

Eiji Nakada · Shinsuke Sugihara · Toshiyuki Kunisada · Toshifumi Ozaki

Received: 4 July 2012 / Accepted: 5 March 2013 / Published online: 12 April 2013

Introduction

For malignant bone and soft-tissue tumors of the forearm, various reconstructions after curative resection have been described [1, 2]. However, amputation is sometimes necessary for complete eradication when the tumors are large or have neurovascular involvement [3]. Resection–replantation is a surgical method for partial limb salvage for upper-extremity malignant tumors [4–8]. Its principle is derived from rotationplasty, and the technique is similar. The tumor-bearing area is resected as a cylindrical segment that includes bone, soft tissues, involved skin, and sometimes vessels and nerves. The distal part of the arm is reimplanted with shortening, adjustment of all structures and, if necessary, vessel anastomosis [4–8]. Resection–replantation is indicated for treating primary malignant tumors of Enneking stage IIB when any other limb-salvage procedures are not indicated and amputation appears to be the only way to achieve wide margins [5, 6]. Although this procedure can retain a relatively functional limb, there have been few reports that describe its long-term results [6, 7]. Here, the long-term result of resection–replantation for mesenchymal chondrosarcoma (MCS) in the distal radius of a 13-year-old boy is presented.

Each author's institution approved the reporting of this case, and all investigations were conducted in conformity with ethical principles of research. The patient was informed that data from the case would be submitted for publication and gave his consent.

E. Nakada (✉) · S. Sugihara
Department of Orthopedic Surgery, Shikoku Cancer Center, Ko-160, Minamiumemoto-cho, Matsuyama city 791-0280, Ehime, Japan
e-mail: eijinakata8522@yahoo.co.jp

T. Kunisada · T. Ozaki
Department of Orthopedic Surgery, Okayama University Hospital, Okayama, Japan

Case report

A 13-year-old boy suddenly developed a mass in the right distal forearm. The patient had no history of recent trauma. However, plain radiographs taken at a local clinic revealed an abnormal lesion in the right distal radius, and he was referred to our institute for further examination. A hard, bony mass was felt in the right distal forearm. A slight tenderness and local heat were noted. Range of motion of the right wrist was slightly restricted. General physical examination, neurological examination, and laboratory data were unremarkable. Plain radiographs demonstrated erosion of the cortex with periosteal reaction and permeative bone destruction in the distal radius (Fig. 1). Computed tomography (CT) revealed a calcifying surface lesion with circumferential involvement of the radius (Fig. 2). Magnetic resonance imaging (MRI) revealed a large lesion of the distal radius with a circumferential extraosseous mass showing isointensity on T1-weighted images and high intensity on T2-weighted images (Fig. 3a, b). Gadolinium-enhanced MRI revealed heterogeneous enhancement (Fig. 3c). Bone scans showed an increased focal uptake at the site of the lesion. Subsequent CT of the chest revealed no metastases. After open biopsy, histological diagnosis was MCS. The patient received neoadjuvant chemotherapy with high-dose methotrexate (MTX), cisplatin (CDDP), Adriamycin (ADM), and ifosfamide (IFO). Two courses of MTX were administered at a dose of 10 g/m^2. Seven days later, the patient received a course of CDDP (120 mg/m^2) and ADM (30 mg/m^2/day × 2 days). After 3 weeks, he

Fig. 1 Periosteal reaction and permeative bone destruction in the distal radius is shown in a preoperative plain radiograph

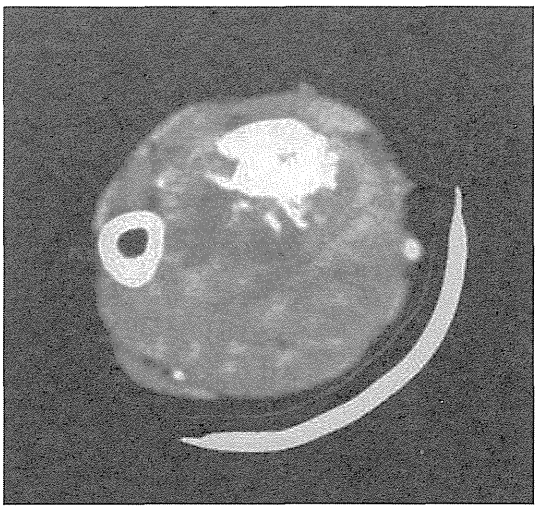

Fig. 2 Calcifying surface lesion and circumferential involvement of the radius is shown on computed tomography

received two courses of IFO (4 g/m^2 on the first day, followed by 2 g/m^2/day × 6 days) with a 3-week interval. MRI after preoperative chemotherapy demonstrated a slight reduction in the extraosseous mass (Fig. 4).

Meticulous surgical planning was performed with the radiological information. A wide margin of 5 cm proximal and distal to the tumor was planned. In this case, the neurovascular bundle was free from tumor, although the size and extensiveness of the tumor made limb salvage difficult with wide resection. For resection–replantation, two circular skin incisions were delineated proximal and distal to the region of the tumor on the midforearm, with sufficient distance from the tumor and including the biopsy scar. A longitudinal extension of the incision was made on the medial and lateral side of the distal forearm (Fig. 5a). The median and ulnar nerves and ulnar artery were carefully exposed by longitudinal skin incisions within the circular incisions and preserved. The superficial radial nerve was sacrificed. The radial artery was exposed and transected proximally and distally. The flexor (flexor carpi ulnaris, flexor carpi radialis, flexor digitorum superficialis, flexor digitorum profundus, palmaris longus, and flexor pollicis longus) and extensor (extensor carpi radialis longus, extensor carpi radialis brevis, extensor digitorum communis, extensor digiti minimi, extensor carpi ulnaris, extensor pollicis longus, extensor pollicis brevis, extensor indicis, and abductor pollicis longus) muscles and tendon groups were transected proximal and distal to the tumor-bearing region. Proximal osteotomy of the radius and ulna at the midforearm level was performed 10 cm from the radial styloid process. A distal disarticulation at the level of the midcarpal joint was also performed, allowing the specimen to be removed (Fig. 5b). The distal ends of the radius and 2nd metacarpal bone were fixed with a plate (Fig. 6). The radial artery and radial cephalic vein were reanastomosed. The median and ulnar nerves were placed in loops between muscles. The extensor (extensor digitorum communis, extensor pollicis longus, extensor pollicis brevis, and abductor pollicis longus) and flexor (flexor digitorum superficialis, and flexor digitorum profundus) tendons and muscles were repaired in place (Fig. 5c). A short-arm splint was applied in the replanted limb. Active and passive range of motion exercises of the fingers were begun 2 and 3 weeks after surgery, respectively. No complications occurred during surgery or the postoperative course. Postoperative chemotherapy was performed with two cycles of MTX, CDP, ADM, and IFO. The patient received two courses of IFO (4 g/m^2 on the first day, followed by 2 g/m^2/day × 6 days) with a 3-week interval. Seven days later, two courses of MTX was administered at a dose of 10 g/m^2, followed by a course of CDDP (120 mg/m^2) and ADM (30 mg/m^2/day × 2 days) after 1 week. Although wide marginal resection was performed, a small lesion appeared 5 cm proximal to the operation scar at 18 months' follow-up; it was resected marginally and histologically determined to be an intravenous metastasis of the MCS.

At 10 years' follow-up, there was no sign of local recurrence or distant metastases. Functional evaluation at the last follow-up was performed according to the criteria of the Musculoskeletal Tumor Society [9], with a score of 30 points (100 %). Although the right forearm was shortened about 10 cm, acceptable appearance and unrestricted function of the hand was achieved. Holding, stabilizing,

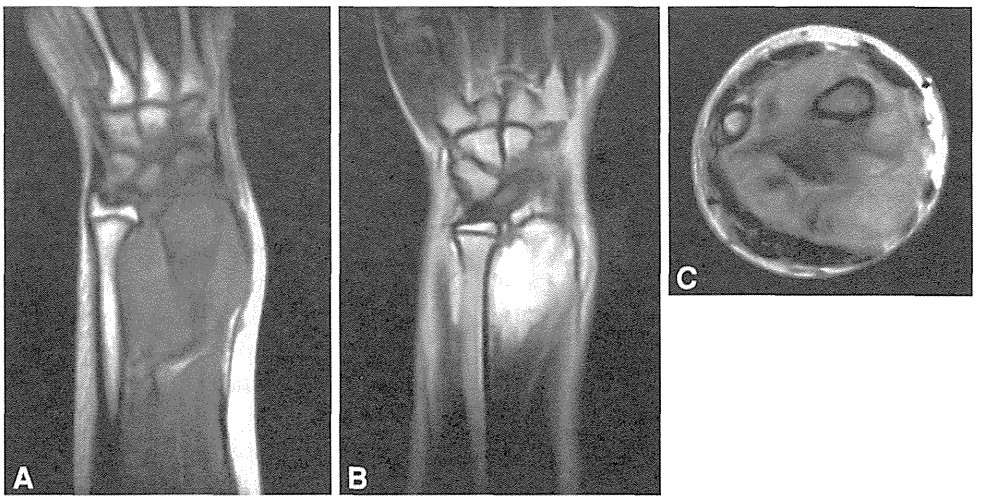

Fig. 3 Magnetic resonance images (MRI) at the first visit demonstrated a large circumferential extraosseous mass of the distal radius that showed **a** isointensity on T1-weighted imaging, **b** high intensity on T2-weighted imaging, and **c** heterogeneous enhancement on gadolinium-enhanced MRI

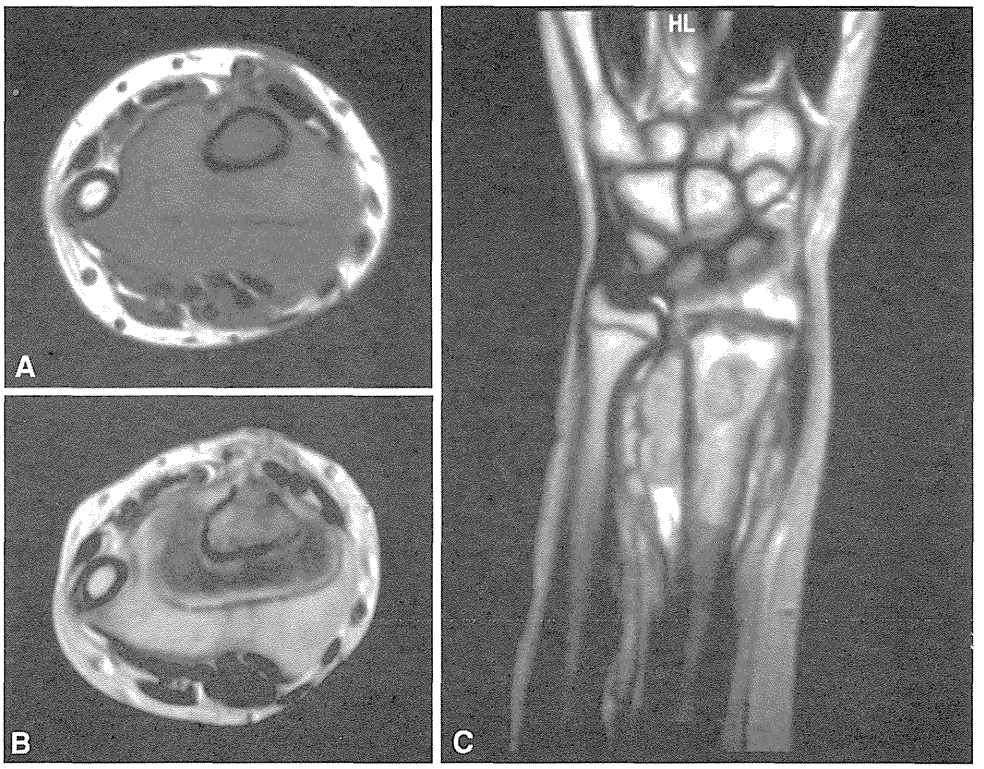

Fig. 4 Magnetic resonance imaging (MRI) after preoperative chemotherapy demonstrated a slight reduction in the extraosseous mass. **a** T1-weighted imaging, **b** T2-weighted imaging, and **c** gadolinium-enhanced MRI

and releasing objects with the affected hand, as well as adequate hand movement (including opposition of the thumb) were also achieved (Fig. 7), as were full range of pronation and supination of the forearm. Tactile sense was partially lost in the dorsal aspect of the thumb, with no accompanying disturbances. A radiograph 4 years and 3 months after surgery showed little change compared with the postoperative one (Fig. 8). At 10 years' follow-up, the patient had no physical handicaps in daily life and was working as an office worker without any problems with writing or operating a computer.

Discussion

Developments in adjuvant therapies, imaging diagnostics, and surgical techniques have made limb-salvage surgery a standard procedure for most primary sarcomas of the upper limbs [10]. However, amputation is sometimes indicated in selected patients with Enneking stage IIB sarcomas in order to achieve wide surgical margins around the tumors for local control [3]. In these circumstances, segmental resection of the tumor-bearing region in a cylindrical fashion and reimplantation of the distal part of the limb for

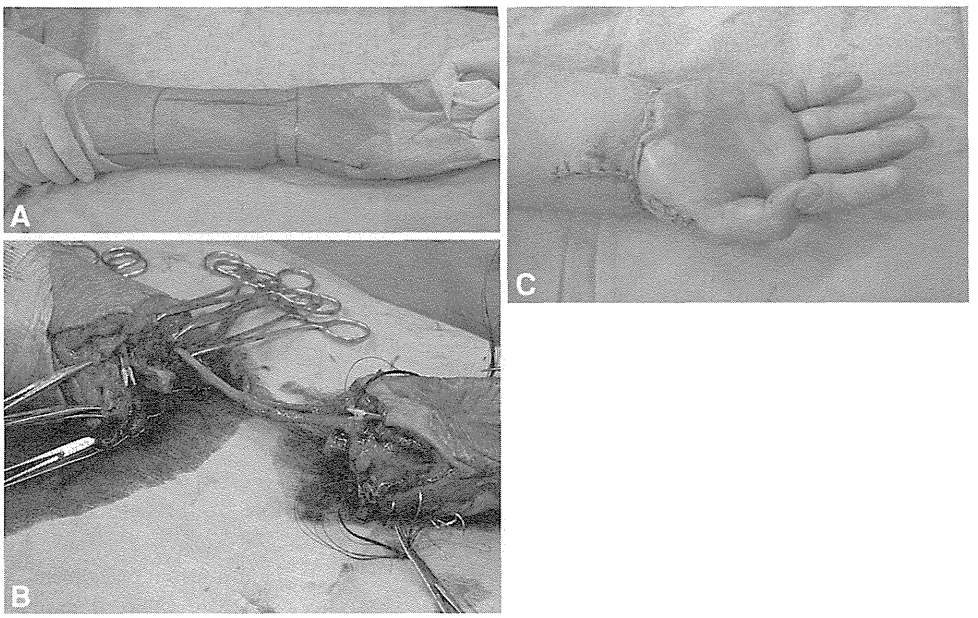

Fig. 5 Surgical procedure: **a** Longitudinal extension of the incision on the medial and lateral side of the distal forearm. **b** Appearance after removal of tumors with soft tissues and bones in the tumor-bearing region excluding the median and ulnar nerves and ulnar artery. **c** Postoperative appearance

Fig. 6 A postoperative anteroposterior and lateral radiograph demonstrated the distal end of the radius and the second metacarpal bone fixed with a plate

limb-function enhancement might be an alternative to amputation [4–8]. At 10 years' follow-up, the patient in this case had an acceptable appearance, unrestricted hand function, no handicaps in daily life, and reported being very satisfied with the treatment outcome. Sparing the major peripheral nerves is thought to be particularly important for patient satisfaction. Windhager et al. [7] suggested that unrestricted hand function can be obtained when the radial, median, and ulnar nerves are spared, allowing excellent hand function. Although the right forearm was shortened about 10 cm, our patient was accepting of the appearance. Windhager et al. [7] suggested that after resection–replantation, cosmetic appearance appears to be of minor importance to the patient as long as function of the shortened limb is satisfactory.

The indication for resection–replantation is treating primary malignant tumors of Enneking stage IIB when any other limb-salvage procedure is not indicated and amputation seems to be the only way of achieving wide resection margins [4–8]. Previous studies of resection–replantation report good local control, with a local cancer recurrence rate of 0–25 % [4–8]. Some studies report that only half of the patients were alive at the last follow-up [5, 7]. This mortality rate might be related to the procedure's inclusion criteria. One of these studies included patients with Stage IIIB sarcomas who had distant metastases [7]. Therefore, patient selection seems to be an important factor in expectations of long-term survival with this procedure. Although our case was a high-grade malignancy, the patient was alive and free from any signs of local recurrence or distant metastases 10 years postoperatively. Resection–replantation may also be useful for treating local recurrence when several compartments have been contaminated by previous inadequate resections [7].

When determining the indication of this procedure, patient characterization is also important [4]. In our opinion, this procedure should be performed for carefully selected and educated patients. Well-supervised rehabilitation should

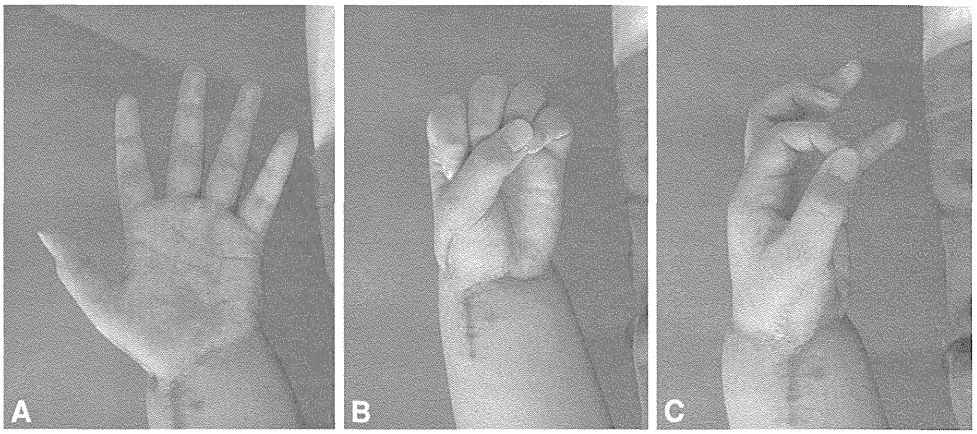

Fig. 7 Postoperative appearance: **a**, **b** Hand movement, and **c** opposition of the thumb were achieved

Fig. 8 Anteroposterior and lateral radiograph 4 years and 3 months after surgery shows the distal end of the radius and the second metacarpal bone fixed with a plate without breakage

be performed to obtain good postoperative function, and the patient should be highly motivated. In this case, the patient was young, and rehabilitation was performed in good course, so unrestricted function of the hand was obtained.

MCS is a rare malignancy for which the effectiveness of adjuvant chemotherapy and radiotherapy is not well defined [11–13]. The prognosis of MCS is poor, with reported 5- and 10-year survival rates of 42–54 % and 20–68 %, respectively [14, 15]. In our case, a neoadjuvant chemotherapy regimen for bone sarcoma was performed, and the tumor responded to the regimen. Although wide resection was performed, intravenous metastasis appeared several centimeters proximal to the operation scar, which was resected marginally. At 10 years' follow-up, the patient was free from local recurrence or distant metastases.

Results in this case indicate that resection–replantation is a reasonable option as a limb-salvage procedure in carefully selected patients with stage IIB primary sarcomas. The procedure can achieve wide surgical margins comparable with amputation and maintain useful hand function that prostheses and amputation cannot achieve. The long-term oncological and functional result was satisfactory in this case. However, this technique can be described only as an alternative in extreme situations in which no other limb-sparing options are indicated. Patient age and characteristics should also be carefully considered.

Conflict of interest Each author certifies no commercial associations (e.g., consultancies, stock ownership, equity interest, patent/licensing arrangements, etc.) that might pose a conflict of interest in connection with the submitted article.

References

1. Innocenti M, Delcroix L, Manfrini M, Ceruso M, Capanna R. Vascularized proximal fibular epiphyseal transfer for distal radial reconstruction. J Bone Joint Surg Am. 2004;86:1504–11.
2. Kesani AK, Tuy B, Beebe K, Patterson F, Benevenia J. Single-bone forearm reconstruction for malignant and aggressive tumors. Clin Orthop Relat Res. 2007;464:210–6.
3. Ghert MA, Abudu A, Driver N, Davis AM, Griffin AM, Pearce D, White L, O'Sullivan B, Catton CN, Bell RS, Wunder JS. The indications for and the prognostic significance of amputation as the primary surgical procedure for localized soft tissue sarcoma of the extremity. Ann Surg Oncol. 2005;12:10–7.
4. Athanasian EA, Healey JH. Resection replantation of the arm for sarcoma: an alternative to amputation. Clin Orthop Relat Res. 2002;395:204–8.
5. El-Gammal TA, El-Sayed A, Kotb MM. Resection replantation of the upper limb for aggressive malignant tumors. Arch Orthop Trauma Surg. 2002;122:173–6.
6. Hahn SB, Choi YR, Kang HJ, Shin KH. Segmental resection and replantation have a role for selected advanced sarcomas in the upper limb. Clin Orthop Relat Res. 2009;467:2918–24.
7. Windhager R, Millesi H, Kotz R. Resection-replantation for primary malignant tumours of the arm. An alternative to forequarter amputation. J Bone Joint Surg Br. 1995;77:176–84.

8. Santori FS, Folliero A, Ghera S, Manili M, Pistolesi R, Monticelli G. Segmental amputation with re-implantation in the treatment of malignant bone tumours of the limbs. Ital J Orthop Traumatol. 1986;12:13–23.
9. Enneking WF, Dunham W, Gebhardt MC, Malawar M, Pritchard DJ. A system for the functional evaluation of reconstructive procedures after surgical treatment of tumors of the musculoskeletal system. Clin Orthop Relat Res. 1993;286:241–6.
10. Barner-Rasmussen I, Popov P, Böhling T, Blomqvist C, Tukiainen E. Microvascular reconstructions after extensive soft tissue sarcoma resections in the upper limb. Eur J Surg Oncol. 2010;36:78–83.
11. Huvos AG, Rosen G, Dabska M, Marcove RC. Mesenchymal chondrosarcoma. A clinicopathologic analysis of 35 patients with emphasis on treatment. Cancer. 1983;51:1230–7.
12. Dantonello TM, Int-Veen C, Leuschner I, Schuck A, Furtwaengler R, Claviez A, Schneider DT, Klingebiel T, Bielack SS, Koscielniak E, CWS study group, COSS study group. Mesenchymal chondrosarcoma of soft tissues and bone in children, adolescents, and young adults: experiences of the CWS and COSS study groups. Cancer. 2008;112:2424–31.
13. Harwood AR, Krajbich JI, Fornasier VL. Mesenchymal chondrosarcoma: a report of 17 cases. Clin Orthop Relat Res. 1981;158:144–8.
14. Nakashima Y, Unni KK, Shives TC, Swee RG, Dahlin DC. Mesenchymal chondrosarcoma of bone and soft tissue. A review of 111 cases. Cancer. 1986;57:2444–53.
15. Dabska M, Huvos AG. Mesenchymal chondrosarcoma in the young. Virchows Arch A Pathol Anat Histopathol. 1983;399:89–104.

日整会誌 (J. Jpn. Orthop. Assoc.) 88：588-594 2014

パネルディスカッション　切除縁評価法の問題点

切除縁評価法の問題点：悪性骨腫瘍*

国定俊之[1]　武田　健[2]　藤原智洋[2]　柳井広之[3]　尾﨑敏文[2]

緒　　言

世界的に標準な切除縁評価法は，Enneking の提唱した surgical margin[1] であるが，wide margin の定義があいまいで，「切除縁が反応層を超えた同一コンパートメント内の正常組織にあるもの」と記載されている．「骨・軟部肉腫切除縁評価法」の巻頭にも記載されているとおり，この Enneking の surgical margin では wide margin の範囲が広く，さらに評価基準は使用上の細則がないため評価するものにより判定が異なる点が問題であった．

そのため日本国内では 1989 年に「骨・軟部肉腫切除縁評価法」が出版され[2]，その後，多くの骨・軟部腫瘍治療専門施設で，この評価法を用いた切除縁の検討が行われてきた．切除縁評価法は，手術材料の切除縁を観察し，実際の切除範囲を明らかにする操作である．切除標本の肉眼的所見を用いて行われ，バリア (barrier) の存在と腫瘍反応層からの距離で総合的に決定される．「骨・軟部肉腫切除縁評価法」では，このようなデータの蓄積があって，初めて画像所見から手術計画を立てることも可能と記載されている．

Key words: Surgical margin, Wide resection, Malignant bone tumor

*Future perspective of surgical margin assessment in the treatment of malignant bone tumor

[1]岡山大学大学院医歯薬学総合研究科運動器医療材料開発講座．Toshiyuki Kunisada: Department of Medical Materials for Musculoskeletal Reconstruction, Okayama University Graduate School of Medicine, Dentistry and Pharmaceutical Sciences

[2]岡山大学大学院医歯薬学総合研究科生体機能再生・再建学講座（整形外科）．Ken Takeda, Tomohiro Fujiwara, Toshifumi Ozaki: Department of Orthopaedic Surgery, Okayama University Graduate School of Medicine, Dentistry, and Pharmaceutical Sciences

[3]岡山大学病院病理診断科．Hiroyuki Yanai: Department of Pathology, Okayama University Hospital

利益相反申告なし

評価法が作成されてから 20 年以上経過しているが，欧米には日本のように統一された評価法はなく，日本の切除縁評価法は世界に誇れる優れた評価法である．しかし，バリアの概念はやや複雑であるため経験が必要なことや，国際的には反応層からの距離ではなく腫瘍からの距離で評価することが一般的であることなど，国際標準となるためにはクリアすべきハードルもある．

評価法の基礎を作成したがん研有明病院が主管である第 46 回日本整形外科学会骨・軟部腫瘍学術集会（松本誠一会長）で，新しい切除縁評価法作成に関するシンポジウムが企画された．本稿では最近の症例を検討して，悪性骨腫瘍の切除縁評価法に関する疑問点・問題点を議論する．

症　　例

2005 年から 2011 年に，岡山大学整形外科で治療した初診時遠隔転移を認めない高悪性度悪性骨腫瘍は 52 例であった．組織型は，骨肉腫 34 例，軟骨肉腫 12 例，Ewing 肉腫 3 例などであった．当科では現在，水平断面 (axial plane) 方向は 2 cm wide margin 以上，長軸方向は 3 cm wide margin 以上での広範切除術を標準治療としている．全例に切除縁評価法による検討を行ってきており，従来の切除縁評価法を用いて判断に迷った点や問題点について考察する．

52 例の切除縁評価は，2 cm wide margin 以上：45 例，1 cm wide margin：4 例，marginal margin 以下：3 例であった．1 cm wide margin となった 4 例は，血管温存目的 (2 例)，および術前化学療法効果著効例での関節温存目的 (2 例) であった．Marginal margin 以下となった 3 例は，骨盤発生，脊椎発生，大腿骨巨大腫瘍であり，広範切除縁確保が困難であった．再発は 4 例に認め，2 cm wide margin：1 例，marginal margin：3 例であった．

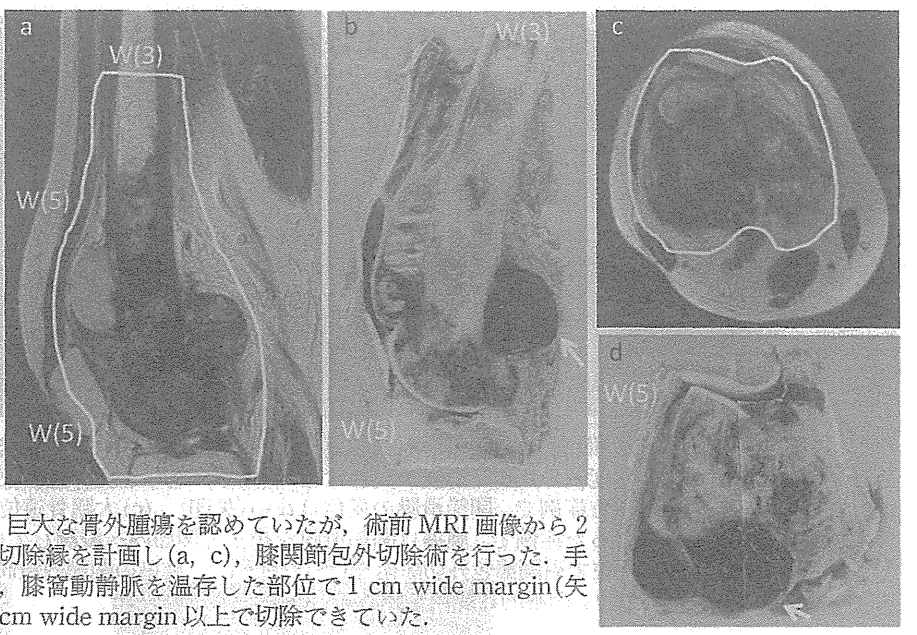

図1 大腿骨遠位部発生骨肉腫．巨大な骨外腫瘍を認めていたが，術前MRI画像から2 cm wide margin: W(2) 以上で切除縁を計画し(a, c)，膝関節包外切除術を行った．手術標本の切除縁評価(b, d)では，膝窩動静脈を温存した部位で1 cm wide margin(矢印)であったが，他の部位では2 cm wide margin以上で切除できていた．

考　　察

1. 断端評価

切除縁評価法は切除標本の縦断割面，横断割面を肉眼的(macroscopic)に観察して行う評価法であり，基本的には腫瘍，もしくは腫瘍反応層からの距離とバリアの概念で決定される．非常にわかりやすい評価法で，手術前の画像検査に容易に適用可能であり，われわれはこの切除縁評価法の概念により手術予定切除縁を計画している．しかし，腫瘍からの距離ではなく反応層からの距離で評価するため，反応層に腫瘍が存在するかしないかで，実際には過少もしくは過大評価されている可能性がある．また，国際的に標準な断端評価法は，R0：断端腫瘍陰性，R1：病理学的(microscopic)に断端腫瘍陽性，R2：肉眼的(macroscopic)に断端腫瘍陽性の分類である．欧米の論文では，病理学的に切除断端と腫瘍の距離を評価して報告されていることが多い[3),4)]．治療成績(再発率や生存率)の検討には，病理学的評価が望ましいが，病理医への負担も大きい．当院でも切除材料2方向の最大割面で，病理学的な断端評価を行っているが，腫瘍からの距離までは評価できていない．また病理学的切除縁評価は，術前画像所見への適用が難しく，手術計画へのフィードバックに問題が残る．手術計画には従来のバリアの概念と反応層からの距離を用いた切除縁評価法を用い，病理学的な断端評価は治療成績を検討する際に用いるのがよいかもしれない．最近の研究会や学会での発表でも，従来の肉眼的な手術標本の切除縁評価(macroscopic)と，病理学的な腫瘍からの距離による切除縁評価(microscopic)が混在してきており，今後は病理学的な切除縁評価も取り入れた基準作成が必要かもしれない．切除縁評価法の表現方法も誤解されやすい．切除縁評価法は最も根治性の低い切除縁で表現すると記載されている．1 cm wide marginと評価された切除縁は，最も腫瘍に近い断端が1 cmであるという意味で，腫瘍全周が1 cm wide marginで切除されていることではない．当科の症例では，1 cm wide marginの4例全例で現在まで再発を認めていない．しかし，これらの症例は2 cm wide marginで手術計画し，血管や関節を温存するためにその周囲のみ1 cm wide marginで切除し，それ以外の切除縁は2 cm wide margin以上で切除している(図1)．切除縁評価の表現は誤解されやすく，注意が必要である．

2. バリア概念：関節内浸潤

バリアの概念については，本シンポジウムではがん研有明病院の阿江先生が問題点と今後の新しい考え方について発表・執筆されている．ここでは，悪性骨腫瘍の切除縁評価として関連がある関節内浸潤について考察する．切除縁評価法では，切除縁が関節内を通過する場合の切除縁評価法として，関節滑膜表面に肉眼的に変色がなければこの部は評価せず，隣接する他の部位で評価する(図2)．つまり，関節滑膜表面に変色がなければ，治癒的切除縁(curative margin)と同等

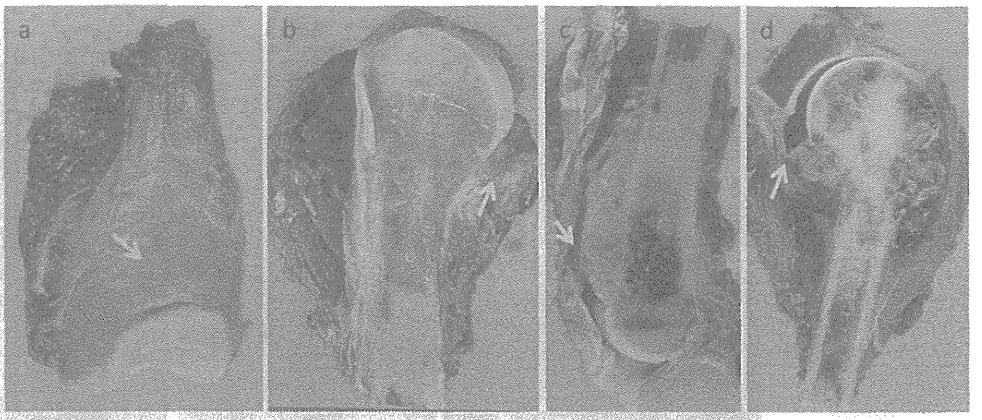

図 2　骨肉腫切除標本での関節滑膜の切除縁評価．(a) 大腿骨遠位部発生で膝関節包内切除術を行った症例で，関節滑膜の変色はない (矢印)．(b) 上腕骨近位部発生で肩関節包内切除術を行った症例で，関節滑膜の変色はない (矢印)．(c) 大腿骨遠位部発生で膝関節包外切除術を行った症例で，腫瘍は関節滑膜を超えて関節内へ浸潤している (矢印)．(d) 上腕骨近位部発生で肩関節包外切除術を行った症例で，腫瘍の関節内浸潤はないが関節滑膜へ浸潤しており，肉眼的に変色を認める (矢印)．

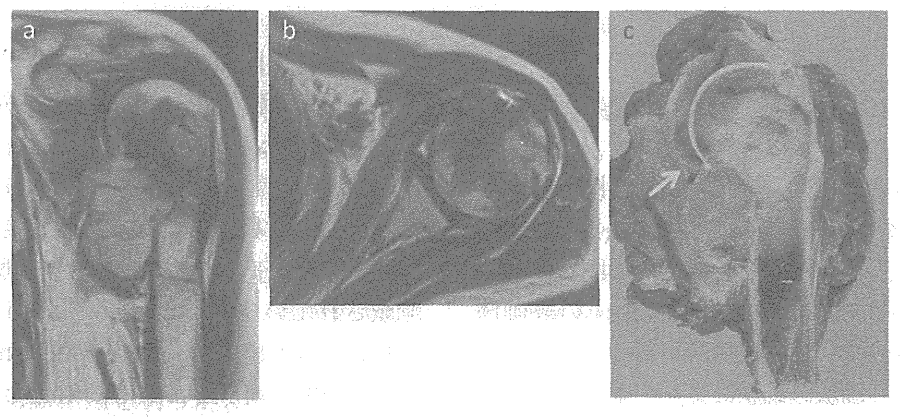

図 3　上腕骨近位部発生骨肉腫．術前 MRI T2 強調画像 (a，b) で関節水腫は認めなかったが，読影所見から関節内浸潤が疑われたため，関節包外切除術を施行．術後の切除縁評価では，関節滑膜に浸潤を認めず，肉眼的にも変色がなく (c)，関節包内切除術でも広範切除縁の確保が可能であった．

の評価である．滑膜の変色があれば辺縁切除縁 (marginal margin)，腫瘍が露出していれば腫瘍内切除縁 (intralesional margin) と評価する．また，「悪性骨腫瘍取扱い規約第 3 版」にも関節滑膜はバリアとして分類されていない．関節滑膜の肉眼的な変色が「ある」「ない」は，術後の切除標本では比較的容易な評価法である．しかし，この変色が「ある」「ない」という肉眼的評価法を術前手術計画に応用することは不可能である．腫瘍が関節滑膜に接していない場合は問題ないが，接している場合には関節内切除術で広範切除縁が確保できるかどうかの判断はできない (図 3)．現在，われわれは関節滑膜を薄い barrier として評価し，術前 MRI 画像で関節液の貯留を認めた場合には，関節液を反応層と考えて関節包外切除術を行い，関節液の貯留がない場合には関節包内切除術を選択している (図 4)．

3. 術前化学療法著効例

原発性悪性骨腫瘍で頻度の高い骨肉腫や Ewing 肉腫は，術前化学療法が標準治療となっている．初診時に巨大な骨外腫瘍を認めていても，術前化学治療が著効すれば腫瘍サイズは縮小し，切除範囲も小さくなる．しかし，切除縁評価法では，術前化学療法が著効した際の切除縁の判定について詳細に決められていない．切除縁評価は術前化学療法後の切除標本で検討するため，術前治療で巨大な腫瘍や広範な反応層が縮小

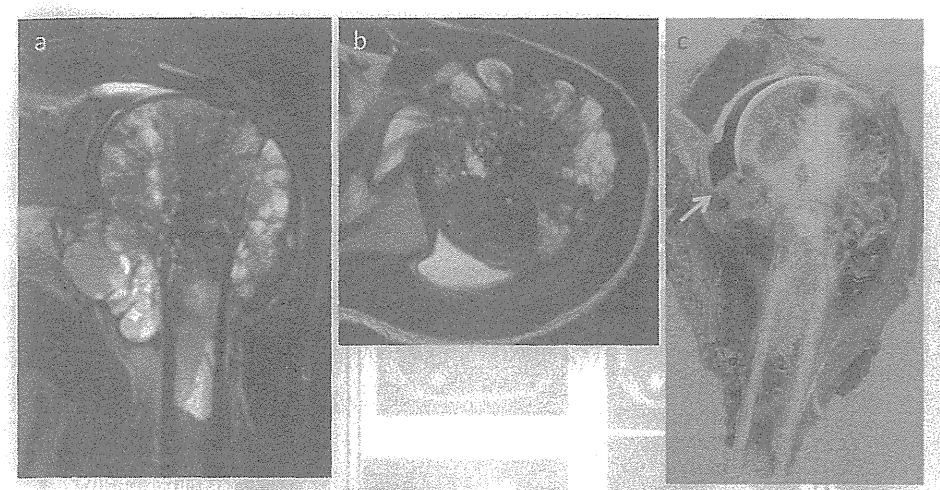

図4　上腕骨近位部発生骨肉腫．術前 MRI T2 強調画像(a, b)で関節水腫を認め，関節内浸潤も疑われたため，関節包外切除術を施行．術後の切除縁評価で関節滑膜(c，矢印)に腫瘍浸潤を認めたが，この部位では関節内への直接浸潤は認めなかった．

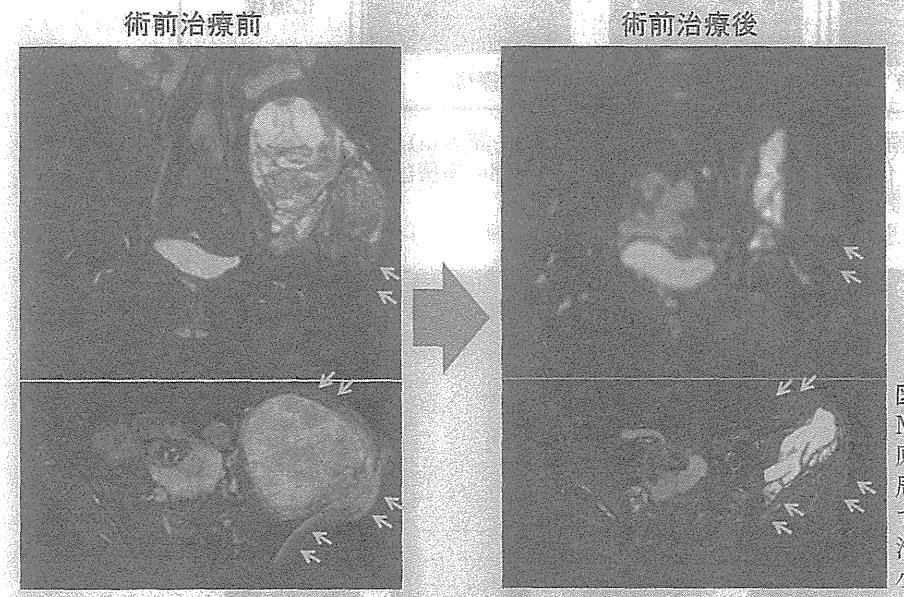

図5　骨盤発生 Ewing 肉腫．治療前の MRI(脂肪抑制 T2 強調画像)では，腸骨原発腫瘍と巨大な骨外腫瘍を認め，腫瘍周囲には広範囲に反応層(浮腫)が進展している．化学療法と放射線治療を行い，治療後の MRI では骨外腫瘍が著明に縮小し，反応層も消失している．

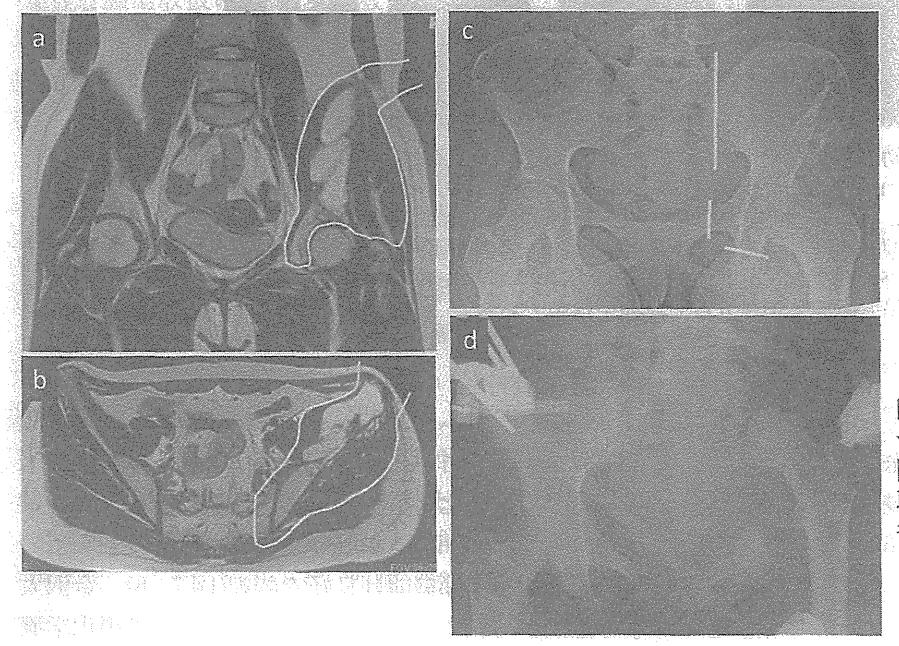

図6　術前治療後の MRI(a, b)で 2 cm wide margin 以上の切除縁を設定．仙腸関節は切除するように仙骨部で骨切し，恥坐骨も 2 cm wide margin で骨切を行った(c)．広範切除術後は，創外固定を用いて再建術を行った(d)．病理学的な術前治療効果判定は，100%壊死であり，切除断端は腫瘍陰性(R0)であった．

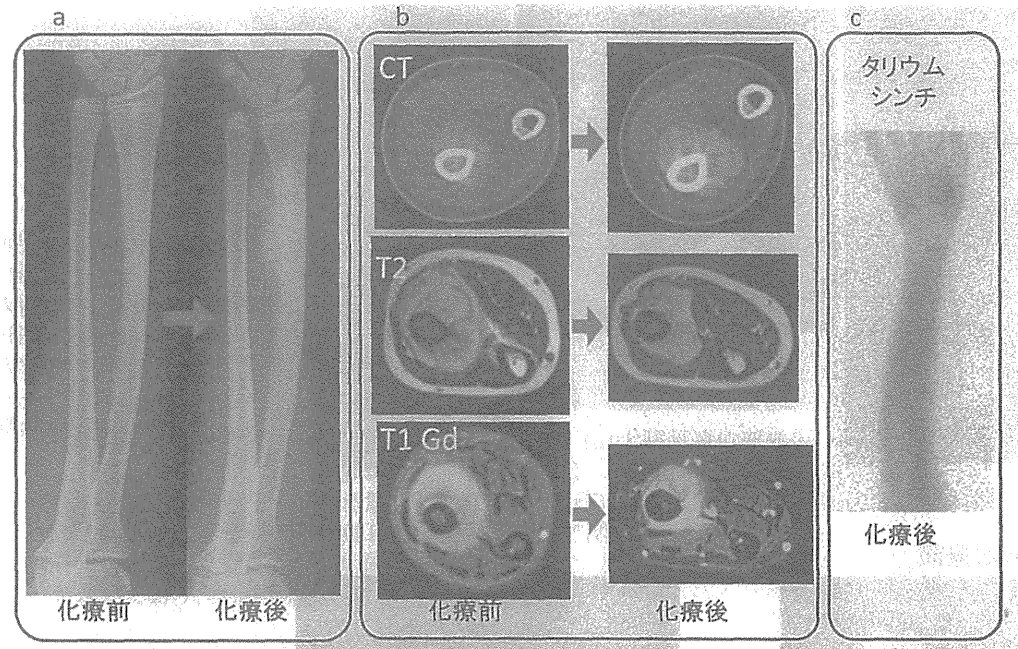

図7　橈骨発生骨肉腫．術前化学療法後に単純X線で硬化像を認め(a)，MRIで腫瘍縮小効果を認めた(b)．さらに，化学療法後のタリウムシンチで腫瘍部の集積は認めず，術前化学療法の抗腫瘍効果は良好と評価した．

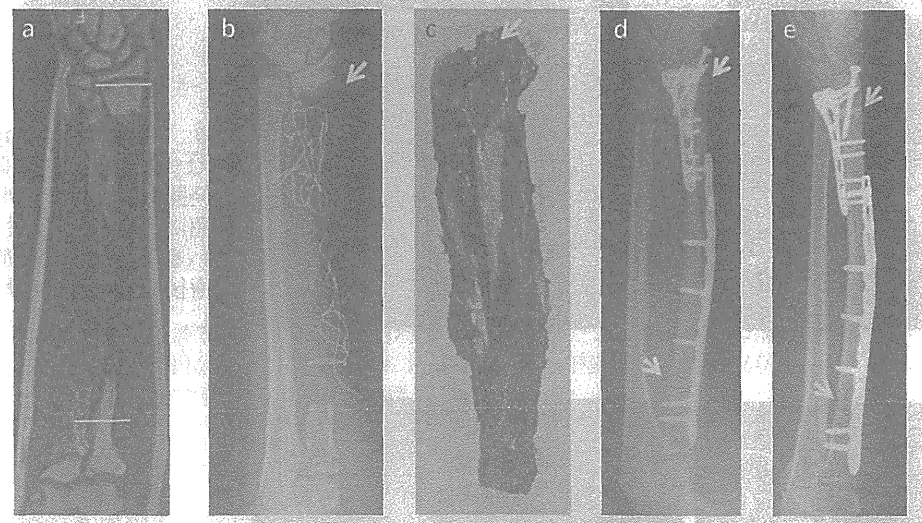

図8　術前化学療法効果が良好であったため，手関節機能を温存するために，橈骨遠位部の骨切りは1 cm wide marginで行い(a：術前橈骨骨切り計画，b：広範切除後の術中単純X線，c：切除標本，矢印：橈骨遠位部骨切り部)，他の部位は2 cm wide margin以上の切除縁を計画した．切除した橈骨を液体窒素処理後に，欠損部に骨移植してプレート固定した(d)．術後8カ月の単純X線(e)で良好な骨癒合を認め(矢印：骨切り部)，術後2年3カ月で無病生存中である．

していれば，縮小した腫瘍や反応層からの切除縁評価となる．化学療法著効例で術前に切除縁を設定する際には，化学療法前には切除すべきであった組織(反応層など)を温存することになる(図5，6)．

2013年5月に開催された第86回日本整形外科学会学術総会で「悪性骨・軟部腫瘍に対する縮小手術」というシンポジウムがあり，術前化学療法が著効した症例では切除縁縮小が可能となる可能性が示唆された．当科では，術前化学療法著効2例に対して，関節温存の目的で1 cm wide marginで骨切を行い，現在まで再発を認めず関節機能は良好である(図7，8)．金沢大学の土屋弘行教授のグループはカフェイン併用化学療